Materials Chemistry and Physics 140 (2013) 398–404

Contents lists available at SciVerse ScienceDirect

Materials Chemistry and Physics

journal homepage: www.elsevier.com/locate/matchemphys

Improved photodegradation activity of TiO_2 via decoration with SnS_2 nanoparticles

Feifei Yang [a], Gaoyi Han [a,*], Dongying Fu [a], Yunzhen Chang [a], Hongfei Wang [b]

[a] Institute of Molecular Science, Key Laboratory of Chemical Biology and Molecular Engineering of Education Ministry, Shanxi University, Taiyuan 030006, PR China
[b] Institute of Optoelectronics, Shanxi University, Taiyuan 030006, PR China

HIGHLIGHTS

- TiO_2 modified with SnS_2 (TiO_2/SnS_2) was synthesized via the hydrothermal method.
- Components of TiO_2 and SnS_2 in composite of TiO_2/SnS_2 exhibit a strong interaction.
- Photodegradation activity of TiO_2 has been improved by SnS_2 on UV or UV–Vis light.

GRAPHICAL ABSTRACT

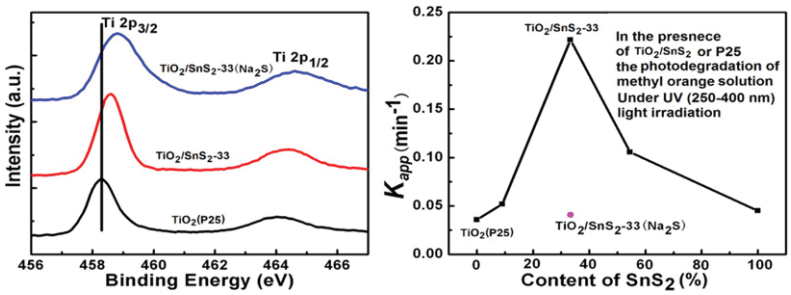

ARTICLE INFO

Article history:
Received 18 October 2012
Received in revised form
14 March 2013
Accepted 19 March 2013

Keywords:
Composite materials
Semiconductors
X-ray photo-emission spectroscopy (XPS)
Electron microscopy (STEM, TEM and SEM)

ABSTRACT

The particles of TiO_2 modified with various amounts of SnS_2 nanoparticles (TiO_2/SnS_2) were synthesized via the hydrothermal method by reacting $SnCl_4 \cdot 5H_2O$ with thioacetamide in 5% (vol.) acetic acid aqueous solution in the presence of TiO_2. The obtained products were characterized by using X-ray diffraction, X-ray photoelectron spectroscopy, UV–Vis diffuse reflection spectra, scanning and transmission electron microscopy. The photodegradation activities of TiO_2/SnS_2 composites have been investigated by using methyl orange as target in water under the light irradiation of 250–400, 360–600 and 400–600 nm. It was found that the photodegradation activity of TiO_2/SnS_2 composites depended on the mass ratio of SnS_2 and the wavelength of the irradiating light. The composites containing 33% SnS_2 exhibited the maximum activity under the light irradiation of 250–400 and 360–600 nm. However, the more SnS_2 in the composites, the higher activity appeared under the irradiation of 400–600 nm light. All the results reveal that the composites possess much better activity than the pristine TiO_2.

1. Introduction

In recent years, TiO_2 nanoparticles have been widely used as an effective photocatalyst in environmental purification in view of its low cost, high activity, chemical and photochemical stability and biocompatibility [1–3]. However, the photocatalytic activity is limited by the wide energy band gap ($E_g \geq 3.2$ eV) and high recombination rate of the photo-induced electron–hole pairs formed in photocatalytic processes [4–8]. Hence, many methods have been employed to prepare nano-sized TiO_2-based catalyst in order to maximize the utilization of the visible light and reduce the recombination of electron–hole [9].

Up to date, it is well known that decorating TiO_2 nanoparticles with some metals, metal ions and semiconductors [10–12] may be a good method to decrease the band gap or to establish energy levels inside the band gap which will lead a significant visible light

* Corresponding author. Tel.: +86 351 7010699; fax: +86 351 7016358.
E-mail address: han_gaoyis@sxu.edu.cn (G. Han).

0254-0584/$ – see front matter © 2013 Elsevier B.V. All rights reserved.
http://dx.doi.org/10.1016/j.matchemphys.2013.03.055

absorption [13–16]. Since there is a suppression of the recombination of electron–hole pairs by coupling two different semiconductors with dissimilar Fermi levels, the introduction of another semiconductor to TiO_2 particles will produce a more efficient separation of the photo-generated electron–hole pairs [17–19].

SnS_2 is a kind of n-type semiconductor with band gap of 2.18–2.44 eV, indicating that it can be used as a promising component in composites to achieve visible-light-responsive ability [20]. According to its electronic property and appropriate matching degree of band potentials with TiO_2, SnS_x/TiO_2 has been synthesized by co-precipitation to enhance the activity of the composites under visible light because the photo-induced electron can transfer from the conduction band of SnS_x to the conduction band of TiO_2 under visible light irradiation [21–23]. Based on the results reported previously, it is expectable that TiO_2/SnS_2 composite with appropriate compositions shall possess higher light-driven photocatalytic activity than individual SnS_2 and TiO_2. However, the TiO_2/SnS_2 composites have only been fabricated by simply mixing the two components or by co-precipitating methods till now and used as photo-catalyst to remove the dye of methyl orange (MO) in water [23].

In this paper, the composites of TiO_2/SnS_2 have been synthesized under hydrothermal condition through reacting $SnCl_4{\cdot}5H_2O$ with thioacetamide (TAA) in the presence of TiO_2. Furthermore, the photodegradation activities of the composites have been investigated in detail and the results show that the synthesized composites exhibit much higher activity than the pristine TiO_2.

2. Experimental

2.1. Materials

TiO_2 (P25) was obtained from Evonik Degussa (Hualisen Guangzhou). $SnCl_4{\cdot}5H_2O$, TAA (99.0%), $Na_2S{\cdot}9H_2O$ (98.0%), CH_3COOH (≥99.5%), MO and other chemicals were of analytical grade and used directly without further purification.

2.2. Synthesis of SnS_2 powder

The samples of $SnCl_4{\cdot}5H_2O$ (2.0 mmol) and TAA (4.0 mmol) were [24] added into a beaker containing 16.0 mL acetic acid aqueous solution (5.0 vol.%) under magnetic stirring, the mixture was then transferred into a 20 mL teflon-lined autoclave after the samples were dissolved. After being heated at 120 °C for 12 h in an oven, the autoclave was cooled naturally to room temperature. The precipitation was collected by centrifugation, washed with deionized water and anhydrous ethanol several times and dried in a vacuum oven at 100 °C for 3 h.

2.3. Synthesis of the nanocomposites of TiO_2/SnS_2

Firstly, TiO_2 powder (200 mg) and certain amounts of $SnCl_4{\cdot}5H_2O$ were dispersed in 8.0 mL acetic acid aqueous solution (5 vol.%) under ultrasonic condition, then 8.0 mL acetic acid aqueous solution containing TAA was dropped into the mixture and the molar ratio of $SnCl_4{\cdot}5H_2O$ and TAA was kept to about 1:2. Subsequently, the mixtures were transferred into teflon-lined stainless steel autoclaves after being stirred 30 min, the teflon-lined autoclaves were then heated at 120 °C for 12 h in an oven. Finally, the products were obtained after the precipitations were filtered, washed with distilled water and anhydrous ethanol several times to remove the impurities, and dried in a vacuum oven at 100 °C for 3 h.

The composites of TiO_2/SnS_2 containing 9.1, 16.7, 23.1, 33.3, 37.5, 50.0, 54.6 wt% of SnS_2 have been synthesized and tested. Under the irradiation of UV and UV–Vis light, the activity of the photocatalysts increased with the increment of SnS_2 in the composites initially, while it decreased when the content of SnS_2 in the composites was larger than 33.3%. In order to make the figures clear, the composites containing 9.1, 33.3 and 54.6 wt% SnS_2 were defined as TiO_2/SnS_2-9, 33 and 54 and the curves corresponding to their photodegradations were listed in the figures.

The SnS_2 particles could be also prepared by using $SnCl_4{\cdot}5H_2O$ and $Na_2S{\cdot}9H_2O$ as raw materials. In order to make a comparison between the two preparation methods, the composite of TiO_2/SnS_2 containing 33.3% SnS_2 named as TiO_2/SnS_2-33(Na_2S) was prepared according to literature [23] by using $SnCl_4{\cdot}5H_2O$ and $Na_2S{\cdot}9H_2O$ as raw materials. Briefly, 10 mL $Na_2S{\cdot}9H_2O$ aqueous solution (0.2 mol L^{-1}) was slowly added into 10 mL $SnCl_4{\cdot}5H_2O$ aqueous solution (0.1 mol L^{-1}) containing appropriate TiO_2 powder under vigorous stirring until the pH of the suspension is about 7. The final product was filtered, washed with distilled water and anhydrous ethanol for several times, and then dried at 100 °C for 3 h under vacuum.

2.4. Characterization

The morphologies of the obtained products were observed by using a scanning electron microscope (SEM, JEOL-JSM-6701F) operating at 10 kV and transmission electron microscope (TEM, JEOL 2010) operating at 200 kV. The XRD patterns of the samples were recorded on a Bruker D8 Advance X-ray diffractometer (Cu Kα). X-ray photoelectron spectroscopy (XPS) measurements were carried out on an ESCAL-ab 220i-XL spectrometer (VG Scientific, England) employing a monochromic Al Ka source at 1486.6 eV, where the binding energies were calibrated by referencing the C1s peak (284.6 eV) to reduce the sample charge effect. The UV–Vis diffuse diffraction spectra were obtained on a Thermo Scientific Evolution 220 UV–Visible spectrophotometer.

2.5. Photocatalytic tests

Photocatalytic activities of the as-prepared products were studied by using the MO solution with a concentration of 20 mg L^{-1} as target under the light irradiation with the wavelength range of 250–400, 360–600 and 400–600 nm. Prior to illumination, 50.0 mL MO aqueous solution containing 10.0 mg of photocatalyst was magnetically stirred in the dark for 30 min to achieve the adsorption/desorption equilibrium between the catalyst and MO. Then the mixture was exposed to the light produced by a 200 W Xe lamp positioned 36 cm away from the vessel, and the temperature was kept at about 25 °C in the process of degradation. During the irradiation, about 1.0 mL of the suspension was taken from the vessel at an interval of 5 or 10 min and the photocatalyst was removed by centrifugation at 12,000 rpm. Then the retained MO in the supernatant solution was analyzed by a UV–Vis spectrophotometer (Varian 50 Bio UV–Visible spectrophotometer) at the maximum absorption wavelength of 462.0 nm. Furthermore, the photodegradation activities of TiO_2 (Degussa P25) and TiO_2/SnS_2-33(Na_2S) synthesized by a precipitation method were also determined under the same conditions with the similar procedure.

The measured absorbance intensities after different irradiation times were transformed to the reduction ratio of MO (*Rrm*), which was calculated using the following expression:

$$Rrm = (A_0 - A_t)/A_0 \times 100\%$$

where A_0 and A_t were the absorbance intensities when illuminated for 0 (that is, just after the dark adsorption) and t min, respectively.

3. Results and discussion

3.1. The characterization of the samples

From the XRD pattern of pure SnS_2 (Fig. 1a) prepared by hydrothermal method, it is found that the characterized diffraction peaks located at 14.93, 28.32, 32.96, 50.09, 52.49, 58.60 and 70.14° are corresponded to the crystal plane of (001), (100), (011), (110), (111), (201) and (113), respectively. The average size of the particles is calculated to be about 7.86 nm and 12.83 nm according to the Debye–Scherrer's formula based on the diffraction peaks of (001) and (110) plane. From the XRD pattern of TiO_2 shown in Fig. 1e, it is found that the diffraction peaks corresponding to anatase phase are located at 25.23, 36.96, 37.03, 53.26, 53.97, 62.55, 68.89, 70.22 and 75.12°. It is notable that the characterized peaks of rutile phase of TiO_2 appear at 27.32, 36.02 and 41.21° at the same time. The XRD patterns of TiO_2/SnS_2 composites with various contents of SnS_2 are shown in Fig. 1b–d, from which it is found that the intensity of diffraction peaks assigned to SnS_2 increases with the increment of the content in the composites. The average size of the SnS_2 in composite of TiO_2/SnS_2-33 is about 5.42 and 9.53 nm based on the (001) and (110) diffraction peaks of SnS_2, respectively, which is obviously smaller than that of pure SnS_2, indicating that the SnS_2 particles can be stabilized by the surface of TiO_2 and that there may be some strong interaction between them. It is surprising to find that the TiO_2/SnS_2-33(Na_2S) composite prepared by reacting $SnCl_4 \cdot 5H_2O$ with $Na_2S \cdot 9H_2O$ in the presence of TiO_2 exhibits only the diffraction peaks of TiO_2 (Fig. 1f), which indicates that the SnS_2 particles dispersed on the surface of TiO_2 are amorphous. This result is consistent with that of the previous literature [21–24].

In order to clarify the interaction between the components in the composites, the XPS spectra are recorded and shown in Fig. 2. It can be seen that the binding energies of $Sn3d_{5/2}$ in SnS_2 and TiO_2/SnS_2-33 are about 486.6 and 486.0 eV, respectively. It is clear that the binding energy of $Sn3d_{5/2}$ in TiO_2/SnS_2-33 is less than that of pure SnS_2 (486.6 eV). Moreover, the XPS peak of $Ti2p_{3/2}$ in sample TiO_2/SnS_2-33 is located at 458.6 eV which is higher than that of TiO_2 (458.3 eV). This may be due to the fact that the Fermi levels of SnS_2 are lower than that of TiO_2, so that the electrons on Ti atom can transfer to the Sn atom in SnS_2 dispersed on the surface of TiO_2, which causes the changes in the outer electron cloud density of Ti and Sn ions and makes the Ti2p binding energy increase and Sn3d binding energy decrease. This fact suggests that there is some intense interactions between TiO_2 and SnS_2 species [25,26]. The XPS peak of $Ti2p_{3/2}$ for TiO_2/SnS_2-33(Na_2S) is located at 458.8 eV which is higher than that of TiO_2 and similar to the result of TiO_2/SnS_2-33. However, the XPS peak of $Sn3d_{5/2}$ centered at 486.7 eV for TiO_2/SnS_2-33(Na_2S) is also higher than that of SnS_2, which may be because some tin oxide has formed during the preparation process of SnS_2 by precipitation and tin oxide may cause the XPS peak shifts to higher region [21].

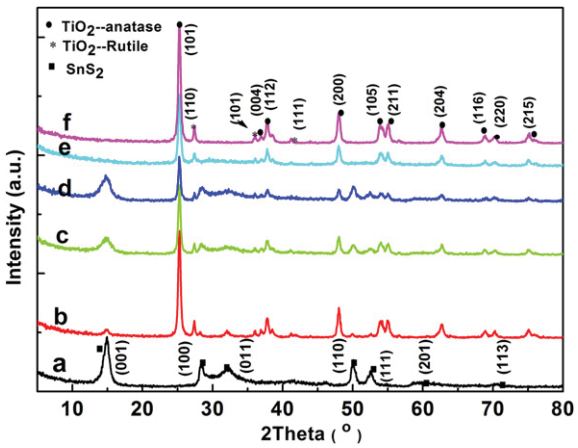

Fig. 1. The XRD patterns of the samples of the pure SnS_2 (a), TiO_2/SnS_2-9 (b), TiO_2/SnS_2-33 (c), TiO_2/SnS_2-54 (d), TiO_2 (e) and TiO_2/SnS_2-33(Na_2S) (f).

From the SEM image shown in Fig. 3A, it is found that the particles in the sample of SnS_2 are aggregated, and that it is difficult to get the shape and size of the particles. From the TEM image shown in Fig. 3D, it is found that the SnS_2 particles are flaky. The particles of TiO_2 have irregular shapes and the size of the particles ranges from 10 to 30 nm (Fig. 3B and E). Furthermore, it is interesting to find that the morphology of TiO_2/SnS_2-33 is between the SnS_2 and TiO_2 profile (Fig. 3C). From the TEM image (Fig. 3F), it can be seen that the surface of TiO_2 has been decorated by some small particles, which indicates that the composites have been synthesized successfully.

Fig. 4 shows the UV–Vis diffuse reflection spectra of the obtained samples. As seen from Fig. 4A, TiO_2 displays an optical absorption capability mainly below 400 nm (Fig. 4A–e), while the pure SnS_2 exhibits not only stronger optical absorption below 400 nm, but also an obvious absorption in the range of 400–650 nm (Fig. 4A–a). It is clear that the absorption spectra of TiO_2/SnS_2 composites have combined the optical absorption features of TiO_2 and SnS_2 (Fig. 4Ab–f). Moreover, the more content of SnS_2 in the composites, the absorption of the composites in the visible region is stronger.

In order to clarify whether the interaction exists between the TiO_2 and SnS_2, the absorption spectrum plotted by adding 67% spectrum of TiO_2 and 33% spectrum of SnS_2 is shown in Fig. 4B–c. It can be seen that the curve c exhibits the same intense of absorption comparing to the samples of TiO_2/SnS_2-33 and TiO_2/SnS_2-33(Na_2S) below 350 nm. However, the composites of TiO_2/SnS_2-33 and TiO_2/SnS_2-33(Na_2S) show much larger light absorption than that of the curve-c in the visible range (Fig. 4B–a, b), and the sample of TiO_2/SnS_2-33 has the largest absorption. This phenomenon also indicates that there is an intense interaction between TiO_2 and SnS_2 species when the samples are prepared by the in-situ synthesis method.

3.2. The photocatalytic activity of samples

By using the MO molecules as the target, the photocatalytic activity of the obtained samples is tested and the results are shown in Fig. 5. From the data shown in Fig. 5A, it is found that the degradation rate is about 33.3% under the UV–Vis (360–600 nm) light for 30 min when 10.0 mg TiO_2 is used as photocatalyst, and is about 62.1% in the presence of TiO_2/SnS_2-33(Na_2S). However, the degradation rate of MO in the presence of TiO_2/SnS_2 prepared by hydrothermal method increases with the increment of SnS_2 initially, while decreases with the increase of SnS_2 content in the composites after the degradation rate reaches the maximum. In the presence of TiO_2/SnS_2-33, the degradation rate under the same condition can reach to about 100% at about 30 min, which is obviously larger than that of TiO_2.

Moreover, it is well accepted that the photo-catalytic degradation of the organic pollutants follows the pseudo first-order kinetic [27], which exhibits a linear relationship between $\ln(C_0/C_t)$ and the reaction time. The kinetics equation of the first-order reaction can be described as:

$$\ln \frac{C_0}{C_t} = Kt \tag{1}$$

where C_0 is the initial concentration of MO, t the reaction time and C_t the concentration of MO at reaction time of t. So based on the

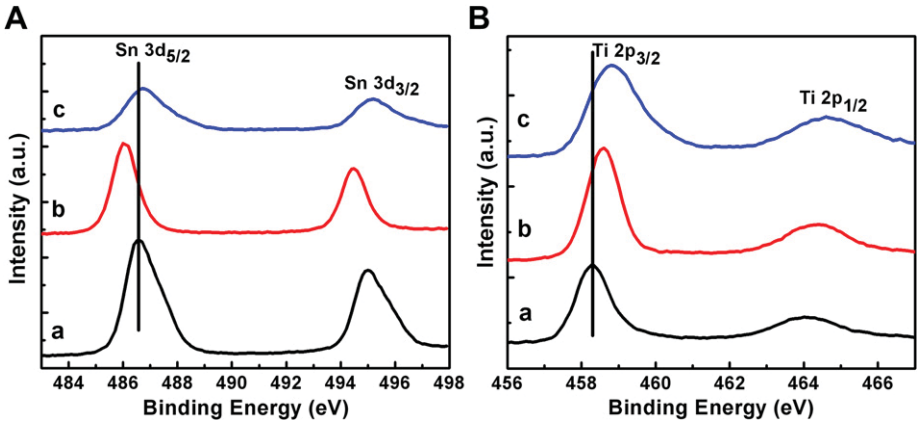

Fig. 2. The XPS spectra of Sn3d (A) and Ti2p (B). The curve of a, b and c is corresponding to the SnS_2, TiO_2/SnS_2-33 and TiO_2/SnS_2-33(Na_2S) in A, while to TiO_2 (P25), TiO_2/SnS_2-33 and TiO_2/SnS_2-33(Na_2S) in B.

first-order equation, the activities of the photocatalysts are determined by measuring the absorbency of the MO in solution at a certain time intervals.

The relationship between the apparent reaction constants (K_{app}) for the photodegradation of MO and the content of SnS_2 in the composites of TiO_2/SnS_2 is shown in Fig. 5B. It can be found that the K_{app} for MO degradation in the presence of TiO_2 is about 0.0135 min^{-1}, and that the K_{app} increases with the increment of SnS_2 in composites initially. The K_{app} reaches the maximum (0.106 min^{-1}) when the content of SnS_2 in the composite is about 33%, which is almost seven times larger than that of TiO_2. However, the K_{app} decreases when the content of SnS_2 in the composites increases further. It can also found that the TiO_2/SnS_2-33(Na_2S) only exhibits a K_{app} of about 0.0225 min^{-1} which is far smaller than that

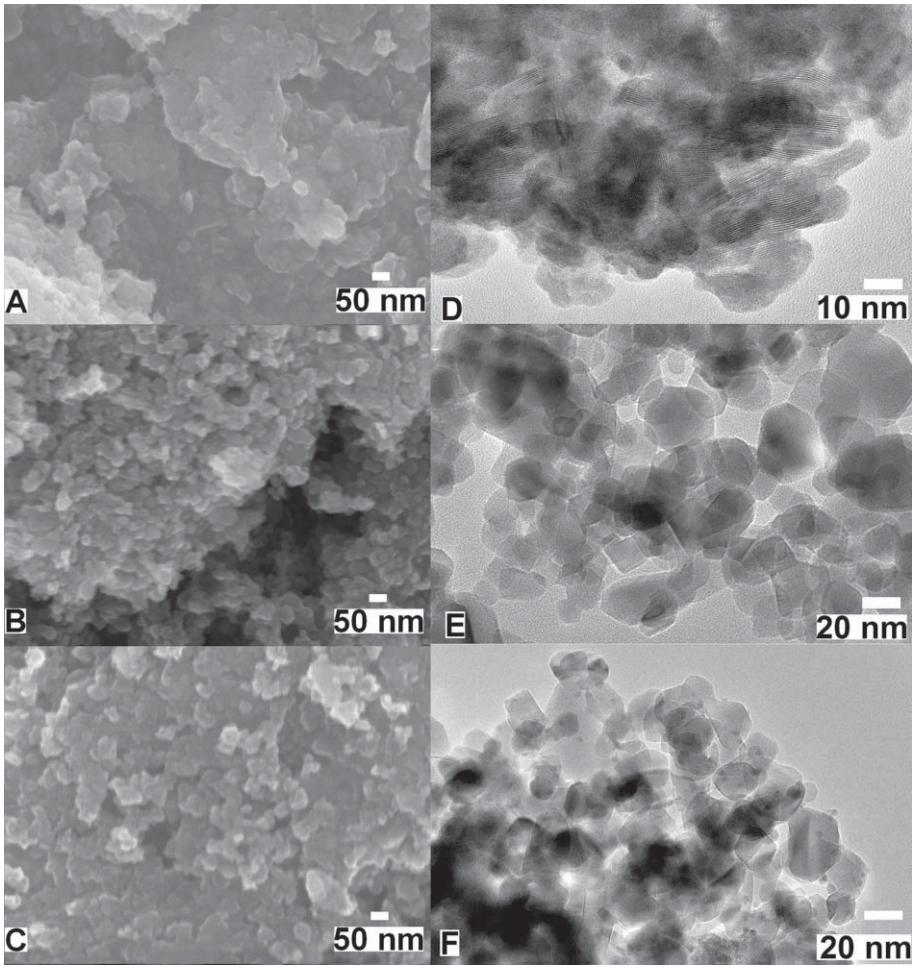

Fig. 3. The SEM images of SnS_2 (A), TiO_2 (B) and TiO_2/SnS_2-33 (C), and the TEM images of SnS_2 (D), TiO_2 (E) and TiO_2/SnS_2-33 (F).

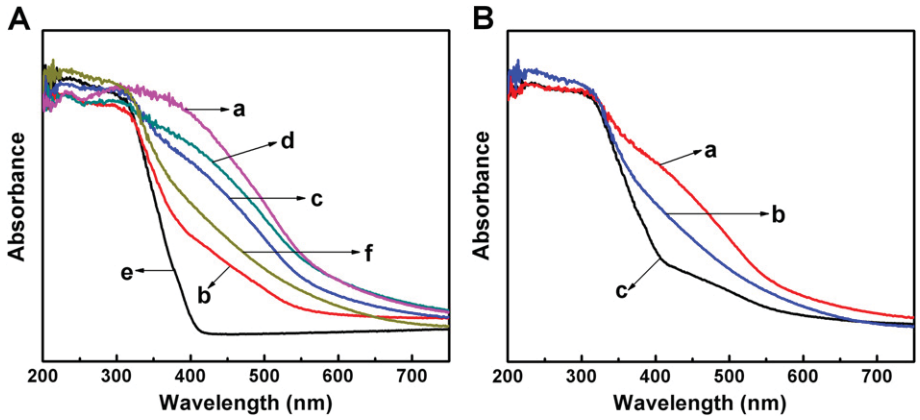

Fig. 4. Diffuse reflection UV–Vis spectra (A) of the samples of SnS_2 (a), TiO_2/SnS_2-9 (b), TiO_2/SnS_2-33 (c), TiO_2/SnS_2-54 (d), TiO_2 (e) and TiO_2/SnS_2-33(Na_2S) (f). (B) The comparison of the UV–Vis spectra of TiO_2/SnS_2-33 (a) and TiO_2/SnS_2-33(Na_2S) (b) and the curve c obtained by adding 67% spectrum of TiO_2 and 33% spectrum of SnS_2.

of TiO_2/SnS_2-33. When the mixture of TiO_2 (6.7 mg) and SnS_2 (3.3 mg) is used as the catalyst to degrade the MO, it is found the degradation rate is about 35.0% at 30 min and the K_{app} for MO degradation is about 0.0137 min^{-1}, which is slightly larger than that of TiO_2. So we can conclude that the composites prepared by hydrothermal method exhibit more activity than the composites prepared by co-precipitation method because of the better crystalline, and that the presence of SnS_2 on the surface of TiO_2 can enhance the photodegradation activity of TiO_2 by improving the separation of the photo-induced electron–hole pairs or by the enhancing of the absorption properties in the visible-light range.

The degradation of MO has also been measured under the light irradiation of 250–400 nm and the results are shown in Fig. 6A and B, from which the similar trend is observed in contrast with Fig. 5A and B. For example, it is found that the degradation rate of MO in presence of TiO_2 is about 70.0% at 30 min, while in the presence of TiO_2/SnS_2-33 it can reach to 100% at 20 min. However, the MO removal over the TiO_2/SnS_2-33(Na_2S) is about 63.9% at the same condition (30 min). The K_{app} for MO degradation in the presence of TiO_2, TiO_2/SnS_2-33 and TiO_2/SnS_2-33(Na_2S) is about 0.0358, 0.222 and 0.0406 min^{-1}. The K_{app} for MO degradation in the presence of TiO_2/SnS_2-33 is five times larger than that of TiO_2, and about four times larger than that of TiO_2/SnS_2-33(Na_2S).

The photodegradation ability of the obtained samples under the light irradiation of 400–600 nm is also been investigated and the results are shown in Fig. 7A and B. As seen from Fig. 7A, the reduction of MO can hardly occur under visible light irradiation in the presence of TiO_2 for a long time (Fig. 7A–e). Instead, the reduction of MO over TiO_2/SnS_2 composites increases with the increment of the SnS_2 content in the composites. For example, in the presence of TiO_2/SnS_2-33 and SnS_2, the degradation rate is about 40% and 98% at 60 min, while in the presence of TiO_2/SnS_2-33(Na_2S), the degradation rate is about 28%. Moreover, it can be seen from the Fig. 7B that in the presence of TiO_2 particles, the system exhibits a K_{app} of about 0.000413 min^{-1}, and that the K_{app} increases with the increment of SnS_2 in the composites of TiO_2/SnS_2, for example, in the presence of TiO_2/SnS_2-33, TiO_2/SnS_2-33(Na_2S) and SnS_2, the K_{app} is measured to be about 0.00857, 0.0058 and 0.0343 min^{-1}. When 3.3 mg SnS_2 is used as photocatalyst, the degradation rate of MO is about 22.2% at 60 min. While the mixture of 6.7 mg TiO_2 and 3.3 mg SnS_2 is used as catalyst, the degradation rate of MO is measured to be about 24.0% at 60 min which is slightly larger than 22.2%, and the K_{app} is calculated to be about 0.00562 min^{-1}. These results are smaller than that of TiO_2/SnS_2-33, indicating that TiO_2 in the composites of TiO_2/SnS_2 can only slightly increase the performance of SnS_2 in the composites.

From all the above results, it can be deduced that the activity improvement of TiO_2 under 360–600 nm light irradiation does not mainly come from the visible light absorption ability of SnS_2 in the composites. According to the literature [25] and XPS spectra, it is considered that the conduction band of the SnS_2 is slightly lower than that of TiO_2, and that the photo-generated electron on SnS_2 is

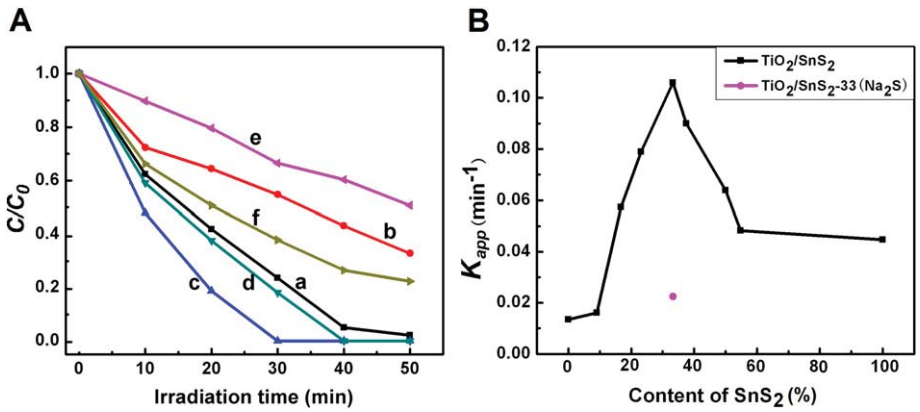

Fig. 5. (A) the plot of C/C_0 versus the time of photodegradation for MO in the presence of (a) SnS_2, (b)TiO_2/SnS_2-9, (c) TiO_2/SnS_2-33, (d) TiO_2/SnS_2-54, (e)TiO_2 and (f) TiO_2/SnS_2-33(Na_2S) under UV–Vis light irradiation (360–600 nm) and (B) The relationships of the apparent reaction constant K_{app} for MO degradation over the composites of TiO_2/SnS_2 with various contents of SnS_2.

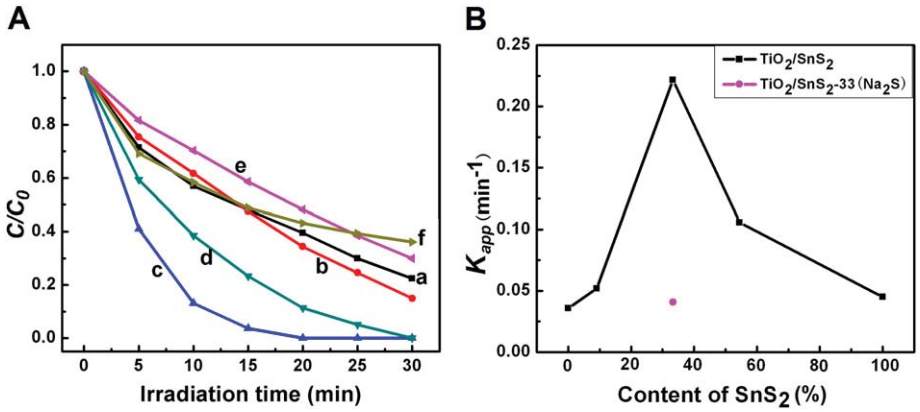

Fig. 6. (A) The plot of C/C_0 versus the time of photodegradation for MO in the presence of (a) SnS_2, (b)TiO_2/SnS_2-9, (c) TiO_2/SnS_2-33, (d) TiO_2/SnS_2-54, (e)TiO_2 and (f) TiO_2/SnS_2-33(Na_2S) under UV light irradiation (250–400 nm) and (B) the relationships of the apparent reaction constant K_{app} for MO degradation over the composites of TiO_2/SnS_2 with various contents of SnS_2.

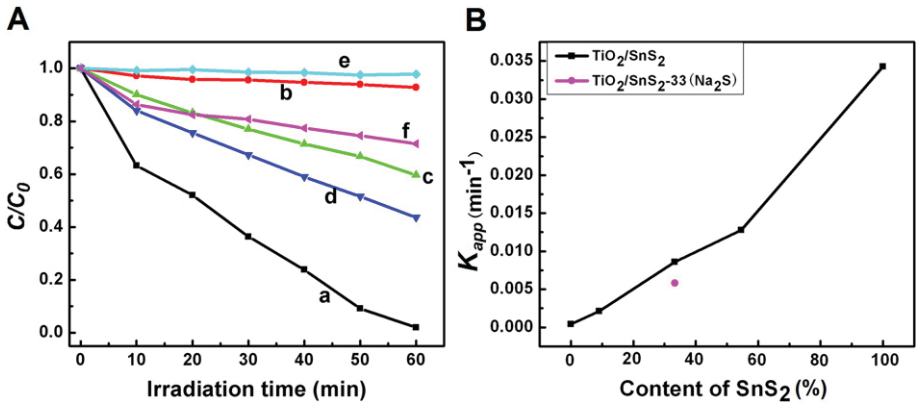

Fig. 7. (A) the plot of C/C_0 versus the time of photodegradation for MO in the presence of (a) SnS_2, (b)TiO_2/SnS_2-9, (c) TiO_2/SnS_2-33, (d) TiO_2/SnS_2-54, (e)TiO_2 and (f) TiO_2/SnS_2-33(Na_2S) under visible light irradiation (400–600 nm) and (B) the relationships of the apparent reaction constant K_{app} for MO degradation over the composites of TiO_2/SnS_2 with various content of SnS_2.

difficult to transfer to TiO_2, so the degradation rate of MO over the composites is smaller than that of pure SnS_2 under 400–600 nm light irradiation. However, the photo-generated electron on TiO_2 can easily transfer to SnS_2 under the 250–400 and 360–600 nm light irradiation, which makes the electron–hole pairs separated and causes the degradation rate of MO to increase dramatically.

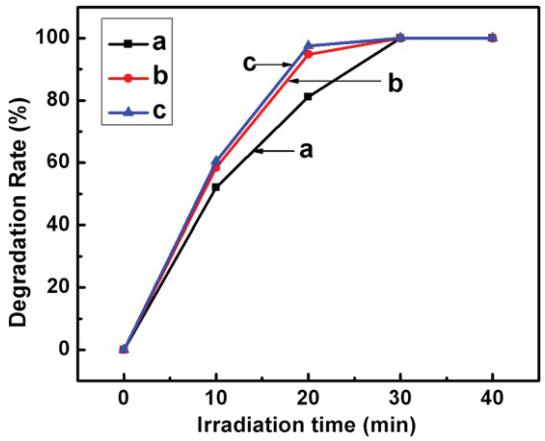

Fig. 8. The degradation rates of MO under irradiation in the presence of TiO_2/SnS_2-33 only (a), in the presence of TiO_2/SnS_2-33 and 1.0 mL isopropyl alcohol (b) and 2.0 mL isopropyl alcohol (c).

In order to clarify the approach of the degradation, the experiments have been carried out by using the isopropyl alcohol as the scavengers for ·OH radicals. In this case, the degradation rate will increase when the degradation of MO is performed by reduction while it will decrease when the degradation is caused by oxidation. From the results shown in Fig. 8, it can be found that the degradation rate of MO increase with the increase of the concentration of the isopropyl alcohol in the mixture, which indicates that the reductive degradation of MO on the TiO_2/SnS_2 surface played a more important role than the oxidative degradation caused by ·OH radicals. This result is similar to the previous literature [28].

4. Conclusions

The composites of TiO_2/SnS_2 have been successfully prepared via a rapid and simple hydrothermal method. The product of TiO_2/SnS_2 with a suitable mass ratio possesses excellent photocatalytic activities under UV or UV–Visible light irradiation. However, under visible (400–600 nm) light irradiation, pure SnS_2 exhibits the better activity. The higher degradation of MO is ascribed to the matching band potentials of TiO_2 and SnS_2 and efficient electron–hole separations via interface. Furthermore, the as-synthesized composites not only show a much better photocatalytic activity toward the degradation of MO in water, but also can be easily recovered from the suspension by filtration or centrifuge after the

use, indicating that they may be a kind of promising photocatalyst in remediation of water polluted by some chemically organic dyes.

Acknowledgments

The authors thank the National Natural Science Foundation of China (21274082, 21073115), the Program for New Century Excellent Talents in University (NCET-10–0926) of China and the Program for the Top Young and Middle-aged Innovative Talents of Shanxi province (TYMIT).

Appendix A. Supplementary data

Supplementary data related to this article can be found at http://dx.doi.org/10.1016/j.matchemphys.2013.03.055.

References

[1] M. Mrowetz, E. Selli, J. Photochem. Photobiol. A: Chem. 180 (2006) 15.
[2] X.F. You, F. Chen, J.L. Zhang, M. Anpo, Catal. Lett. 102 (2005) 247.
[3] N. Barka, S. Qourzal, A. Assabbane, A. Nounah, Y. Ait-Ichou, J. Photochem. Photobiol. A 195 (2008) 346.
[4] M. Bowker, D. James, P. Stone, R. Bennett, N. Perkins, L. Millard, J. Greaves, A. Dickinson, J. Catal. 217 (2003) 427.
[5] C. Young, T.M. Lim, K. Chiang, J. Scott, R. Amal, Appl. Catal. B 78 (1–2) (2008) 1.
[6] T.G. Schaaff, D.A. Blom, Nano Lett. 2 (2002) 507.
[7] C.B. Zhang, H. He, K. Tanaka, Appl. Catal. B 65 (1–2) (2006) 37.
[8] H. Einaga, T. Ibusuki, S. Futamura, Environ. Sci. Technol. 38 (2004) 285.
[9] D.S. Wang, J. Zhang, Q.Z. Luo, X.Y. Li, Y.D. Duan, J. An, J. Hazard. Mater. 169 (2009) 546.
[10] Y.J. Zhang, W. Yan, Y. Wu, P. Zhen, H. Wang, Mater. Lett. 23 (2008) 3846.
[11] M.R. Hoffmann, S.T. Martin, W. Choi, D.W. Bahnemann, Chem. Rev. 95 (1995) 69.
[12] Y.H. Xu, Z.X. Zeng, J. Mol. Catal. A: Chem. 279 (2008) 77.
[13] T. Ivanova, A. Harizanova, M. Surtchev, Z. Nenova, Sol. Energy Mater. Sol. C 76 (2003) 591.
[14] D. Mardare, P. Hones, Mater. Sci. Eng. B 68 (1999) 42.
[15] W. Choi, A. Termin, M.R. Hoffmann, J. Phys. Chem. 98 (1994) 13669.
[16] H. Zhang, S. Ouyang, Z. Li, L. Liu, T. Yu, J. Ye, Z. Zou, J. Phys. Chem. Solids 67 (2006) 2501.
[17] S.K. Zheng, T.M. Wang, W.C. Hao, R. Shen, Vacuum 65 (2002) 155.
[18] Y. Cao, W. Yang, W. Zhang, G. Liu, P. Yue, New J. Chem. 2 (2004) 218.
[19] F.B. Li, X.Z. Li, M.F. Hou, Appl. Catal. B: Environ. 48 (2004) 185.
[20] X.L. Gou, J. Chen, P.W. Shen, Mater. Chem. Phys. 93 (2005) 557.
[21] Y.C. Zhang, Z.N. Du, K.W. Li, M. Zhang, D.D. Dionysiou, ACS Appl. Mater. Interfaces 3 (2011) 1528.
[22] J. Zeng, R. Li, S. Liu, L. Zhang, ACS Appl. Mater. Interfaces 3 (2011) 2074.
[23] C.Y. Yang, W.D. Wang, Z.C. Shan, F.Q. Huang, J. Solid State Chem. 182 (2009) 807.
[24] Y.C. Zhang, Z.N. Du, K.W. Li, M. Zhang, Sep. Purif. Technol. 81 (2011) 101.
[25] B.F. Xin, D.D. Ding, Y. Gao, X.H. Jin, H.G. Fu, P. Wang, Appl. Surf. Sci. 255 (2009) 5896.
[26] V.B.R. Boppana, R.F. Lobo, J. Catal. 281 (2011) 156.
[27] Y.J. Li, X.D. Li, J.W. Li, J. Yin, Water Res. 40 (2006) 1119.
[28] X. Li, J. Zhu, H.X. Li, Appl. Catal. B: Environ. 123-124 (2012) 174.